Ordered mesoporous Co_3O_4 as highly active catalyst for low temperature CO-oxidation†

Harun Tüysüz, Massimiliano Comotti and Ferdi Schüth*

Received (in Cambridge, UK) 27th May 2008, Accepted 10th July 2008
First published as an Advance Article on the web 25th July 2008
DOI: 10.1039/b808815b

Cubic ordered mesoporous Co_3O_4, prepared *via* the nanocasting pathway using KIT-6 as hard template, was found to be an excellent catalyst for low temperature CO oxidation, with the activity clearly depending on surface area and pore systems of the catalysts.

Since the introduction of the nanocasting[1] (hard templating) pathway, increasing efforts have been devoted to the preparation of ordered mesoporous metal oxides such as Co_3O_4,[2–4] Cr_2O_3,[5,6] CeO_2,[7] MgO,[8] Fe_3O_4[9] and ferrihydrite.[10] These materials have high surface area compared to bulk materials, and therefore can be used as efficient catalyst supports and as catalysts themselves. Low temperature CO oxidation is very important in many applications including air purification and pollution control devices, automotive emission control, gas purification of the hydrogen to feed PEM fuel cells, closed-cycle CO_2 lasers and CO gas sensors.[11] Although the most often studied materials for low temperature CO oxidation are gold based catalysts[12–14] several studies have also used Co_3O_4 (bulk or supported) which shows a very high activity for this reaction as well.[15–19] Depending on the preparation method for the materials and the reaction conditions, Co_3O_4 shows different activity in CO oxidation. Recently Wang *et al.* reported catalytic activity of a series of Co_3O_4 samples,[20] and they showed that CO conversion of the samples can reach 100% at ambient temperature and even below, using a gas mixture consisting of 0.5 vol% CO, 14.4 vol% O_2, and 85.1 vol% N_2 with a total flow rate of 20 mL min^{-1}, corresponding to a space velocity of 4000 mL g_{cat}^{-1} h^{-1}. Deactivation was observed to be severe, and reliable activities of the catalysts could not be extracted from the data, since the experiments were carried out at full conversion, and the deactivation patterns did not show consistent trends. Haruta's group has reported light-off temperatures (temperature of 50% conversion, T_{50}) as low as −54 °C under conditions close to the ones used in our study, but only if the reaction gas was meticulously dried. At normal operation, the T_{50} was around 40 °C.[21]

Since the nanocasting pathway allows the synthesis of highly defined pore systems and the generation of high surface areas, we studied the catalytic activity of nanocast Co_3O_4 in CO-oxidation and the dependence of the catalytic activity on the porosity of the samples. Ordered mesoporous Co_3O_4 with different textural parameters was prepared *via* the nanocasting pathway. The catalytic performance of these materials was in the same range as that of the best reported materials with respect to conversion at room temperature, but a more precise comparison is difficult due to the different conditions used in previous publications.

Cubic ordered mesoporous silica (KIT-6) was synthesized according to the literature.[22] The pore size of the KIT-6 was varied by changing the aging temperature (40, 100 and 135 °C). With increasing aging temperature during the hydrothermal process, pore size and pore volume of the synthesized KIT-6 increase while silica wall thickness decreases. KIT-6 was used as a hard template to fabricate ordered mesoporous Co_3O_4. Briefly, 0.5 g of KIT-6 was dispersed in 5 ml of 0.8 M $Co(NO_3)_2{\cdot}6H_2O$ in ethanol and stirred for 1 h at room temperature, followed by evaporation of the ethanol at 50 °C. The composite was calcined at 200 °C for 6 h. The material was re-impregnated again, followed by calcination at 450 °C for 6 h. The silica template was then removed by leaching with 2 M NaOH aqueous solution. Finally, the resulting Co_3O_4 was washed several times with water and then dried at 50 °C. All samples were characterized by nitrogen-sorption, X-ray diffraction, (XRD), transmission electron microscopy (TEM) and high resolution scanning electron microscopy (HR-SEM). The activities of the catalysts for CO oxidation were measured in a plug flow reactor using 200 mg of catalyst (250–500 μm size fraction) in a gas mixture of 1 vol% CO in air (Air Liquide, 99.997% purity) at a flow rate of 60 mL min^{-1}, corresponding to a space velocity of 18 000 mL g_{cat}^{-1} h^{-1}. Temperatures during these tests were ramped at 2 °C min^{-1} while CO conversion was recorded. Control experiments proved that this transient operation gives the same activity as a steady state measurement of activity. For clarification, the samples were labelled as Co_3O_4-T, with T representing the aging temperature of the hard template.

The structure and porosity of nanocast Co_3O_4 strongly depend on the parameters of the nanocasting process, and the results of a detailed study will be reported elsewhere,[23] since this would exceed the scope of this contribution. In summary, Co_3O_4-40 which had been fabricated from KIT-6 aged at low temperature has uncoupled sub-frameworks while Co_3O_4-100 and Co_3O_4-135 have a coupled framework. The parent material aged at higher temperature contains a high fraction of micropores connecting the two mesopore systems.

Max-Planck-Institut für Kohlenforschung, Kaiser-Wilhelm-Platz 1, Mülheim an der Ruhr, 45470, Germany. E-mail: schueth@mpi-muelheim.mpg.de; Fax: +49 208 306 2995; Tel: +49 208 306 2373

† Electronic supplementary information (ESI) available: Fig. S1. Deactivation plot for Co_3O_4-40 catalyst. Fig. S2, XPS spectrum for Co_3O_4-100 before and after catalytic test. See DOI: 10.1039/b808815b

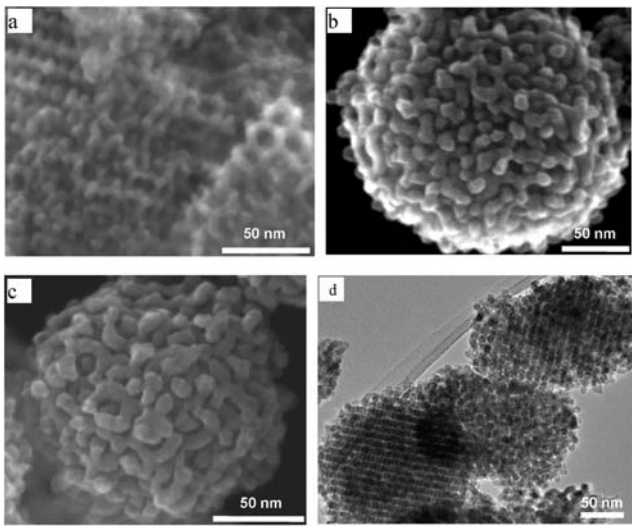

Fig. 1 HR-SEM images of Co_3O_4 which was nanocast from KIT-6 with 40 (a), 100 (b) and 135 (c) °C aging temperature. Fig. 1d shows a TEM image of Co_3O_4-100 after catalytic testing.

This leads to concerted accretion of the cobalt-material in the same sample regions.[23] This phenomenon can be seen clearly from HR-SEM images of Co_3O_4-40 (Fig. 1a–c). Both pore systems of the mesoporous Co_3O_4-100 and Co_3O_4-135 are interpenetrating, resulting in a rather dense structure. Textural parameters of the Co_3O_4 samples were determined before and after CO oxidation by N_2-sorption and the results are given in Table 1. As one can see from Table 1, Brunauer–Emmett–Teller (BET) surface area, pore volume and pore size of the nanocast Co_3O_4 decrease with increasing aging temperature of the silica template. The textural parameters were not significantly affected by the catalytic test.

Catalytic activities of the samples at different temperatures are given in Fig. 2. As one can see, the light-off temperature of the CO (T_{50}) increases with decreasing surface area of the ordered mesoporous Co_3O_4. T_{50} for Co_3O_4-40 is 4 °C while for Co_3O_4-100 and Co_3O_4-135 it is 38 and 91 °C, respectively. The shallower slope of the conversion curve especially for the Co_3O_4-135 sample may indicate the onset of pore diffusion limitations in the very narrow pore system on the particle level in the materials with interpenetrating Co_3O_4 frameworks. This notion is also supported by the fact that the catalytic activity normalized to surface area is not constant, but highest for Co_3O_4-40. This catalyst with an uncoupled sub-framework structure (high surface area) shows very high activity for CO oxidation at low temperature, in the same range as observed for very good gold based catalysts. Full conversion is reached already at room temperature with this material, while the lowest activity sample shows hardly any conversion at this temperature, although the surface area is only a little bit more

Table 1 N_2-Sorption results of Co_3O_4 before and after (in brackets) catalytic test

	BET/m^2 g^{-1}	Pore volume/cm^3 g^{-1}	Pore size/nm
Co_3O_4-40	153 (157)	0.479 (0.480)	6.0 (6.0)
Co_3O_4-100	114 (111)	0.189 (0.189)	3.3 (3.3)
Co_3O_4-135	70 (68)	0.110 (0.106)	3.0 (3.0)

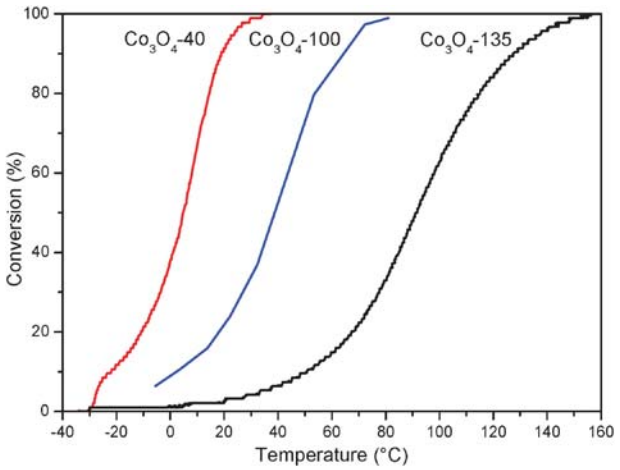

Fig. 2 Conversion as a function of temperature for CO oxidation over Co_3O_4 samples (200 mg catalyst, space velocity of 18 000 mL g_{cat}^{-1} h^{-1}).

than a factor of two lower.

Co_3O_4 is known to suffer from deactivation, and thus deactivation profiles for these materials have also been determined at constant temperature. In agreement with literature data, the materials described here are also deactivated with time-on-stream. A quasilinear deactivation profile was recorded, for instance, for Co_3O_4-40 which shows a reduction of the conversion from about 85% to *ca.* 43% conversion at 15 °C over 4 h. (For the time profile of the deactivation, see ESI Fig. S1.†)

Since the textural parameters of the materials do not change during the catalytic test (Table 1), this loss of activity cannot be attributed to reduction of the surface area. Also the structures show pronounced changes during the catalytic test neither on the mesoscale nor on the atomic scale, as revealed in low and wide angle XRD patterns (Fig. 3). The low angle

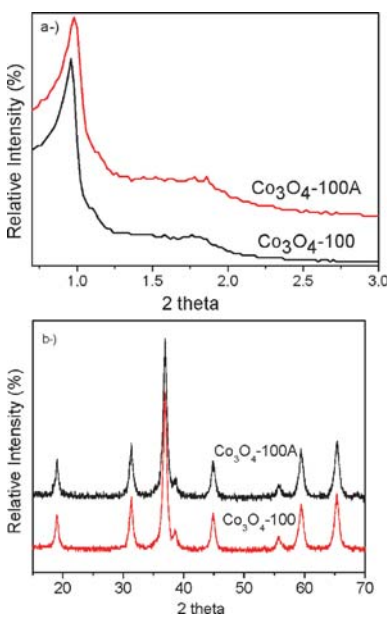

Fig. 3 Low angle (a) and wide angle (b) XRD patterns of Co_3O_4 before and after catalytic test (Co_3O_4-100A).

XRD pattern of the sample still indicates the presence of the ordered mesostructure, while the wide angle XRD pattern shows the pure Co_3O_4 spinel phases before and after CO oxidation, with no significant changes of the peak width, indicating unchanged domain sizes. The well preserved structure of the Co_3O_4 after the CO oxidation can also be seen from the TEM image (Fig. 1d). From these analyses it can be concluded that the deactivation phenomenon is not caused by a structural or textural modification of the material when exposed to reaction conditions. It is thus probably rather the surface chemistry of the materials which is changed. This could be a local change of oxidation state or surface structure, which is not detected by the bulk techniques used for the analysis of the samples. In order to check a possible change of oxidation state or surface contamination, XPS studies of fresh and used catalyst were carried out. The spectra did not reveal any change in the XPS patterns (see ESI, Fig. S2†). However, since we could not remove the sample from the reactor without exposure to air due to the construction of the reactor, the spectrum after reaction may not be truly representative of the aged catalyst under reaction conditions. Further studies will thus be necessary to clarify the origin of the deactivation process.

To summarize, we have synthesized a series of ordered mesoporous Co_3O_4 sample *via* the hard templating pathway and tested them in the CO oxidation reaction. Co_3O_4 with high surface area is sufficiently active to convert 100% CO to CO_2 around room temperature even at a space velocity of 18 000 mL g_{cat}^{-1} s^{-1}. The activity is clearly dependent on the textural properties of the samples, with the best performance achieved for the material with the highest surface area and the most open pore system. The catalysts lose about 50% of their activity over 4 h during the reaction. However, this is not due to structural breakdown or loss of surface area. Since the ordered structure of the Co_3O_4 is stable under the reaction conditions, this kind of ordered mesoporous materials can be used as support and catalyst. Further work related to the deposition of gold nanoparticles into Co_3O_4 and investigation of the catalytic activity of these materials in CO oxidation is in progress in our laboratory, since this may lead to catalysts exploiting both the exceptional activity for CO oxidation of the gold and the Co_3O_4 support material.

This work was supported partially by the Leibniz Program of the DFG and DFG SFB 558. We thank C. Lehmann, B. Spliethoff and H. Bongard for the TEM and HR-SEM images and C. Weidenthaler for XPS measurements.

Notes and references

1 R. Ryoo, S. H. Joo and S. Jun, *J. Phys. Chem. B*, 1999, **103**, 7743.
2 B. Z. Tian, X. Lui, L. Solovyov, Z. Liu, H. Yang, Z. Zhang, S. Xie, F. Zhang, B. Tu, C. Yu, O. Terasaki and D. Zhao, *J. Am. Chem. Soc*., 2004, **126**, 865.
3 Y. Wang, C. M. Yang, W. Schmidt, B. Spliethoff, E. Bill and F. Schüth, *Adv. Mater*., 2005, **17**, 53.
4 W. Yue, A. H. Hill, A. Harrison and W. Zhou, *Chem. Commun*., 2007, 2518.
5 B. Tian, X. Lui, H. Yang, S. Xie, C. Yu, B. Tu and D. Zhao, *Adv. Mater*., 2003, **15**, 1370.
6 K. Jiao, B. Zhang, B. Yue, Y. Ren, S. Liu, S. Yan, C. Dickinson, W. Zhou and H. He, *Chem. Commun*., 2005, 5618.
7 S. Laha and R. Ryoo, *Chem. Commun*., 2003, 2138.
8 J. Roggenbuck and M. Tiemann, *J. Am. Chem. Soc*., 2005, **127**, 1096.
9 F. Jiao, J. C. Jumas, M. Womes, A. V. Chadwick, A. Harrison and P. G. Bruce, *J. Am. Chem. Soc*., 2006, **128**, 12905.
10 H. Tüysüz, E. L. Salabas, C. Weidenthaler and F. Schüth, *J. Am. Chem. Soc*., 2008, **130**, 280.
11 C. W. Corti, R. J. Holliday and D. T. Thompson, *Top. Catal*., 2007, **44**, 331.
12 A. Stephen, K. Hashmi and G. J. Hutchings, *Angew. Chem., Int. Ed*., 2006, **45**, 7896.
13 M. Comotti, W. Li, B. Spliethoff and F. Schüth, *J. Am. Chem. Soc*., 2006, **128**, 917.
14 M. Haruta, N. Yamada, T. Kobayashi and S. Iijima, *J. Catal*., 1989, **115**, 301.
15 Y. Y. Yao, *J. Catal*., 1974, **33**, 108.
16 M. Haruta, S. Tsubota, T. Kobayashi, H. Kageyama, M. J. Genet and B. Delmon, *J. Catal*., 1993, **144**, 175.
17 J. Jansson, *J. Catal*., 2000, **194**, 55.
18 P. Broqvist, I. Panas and H. Persson, *J. Catal*., 2002, **210**, 198.
19 J. Jansson, A. E. C. Palmqvist, E. Fridell, M. Skoglundh, L. Österlund, Peter, Thormählen and V. Langer, *J. Catal*., 2002, **211**, 387.
20 Y. Z. Wang, Y. X. Zhao, C. G. Ga and D. S. Liu, *Catal. Lett*., 2007, **116**, 136.
21 D. A. H. Cunningham, T. Kobayashi, N. Kamijo and M. Haruta, *Catal. Lett*., 1994, **25**, 257.
22 F. Kleitz, S. H. Choi and R. Ryoo, *Chem. Commun*., 2003, 2136.
23 H. Tüysüz, C. W. Lehmann, H. Bongard, R. Schmidt, B. Tesche and F. Schüth, *J. Am. Chem. Soc*., 2008, DOI: 10.1021/ja803362s.

